

# **Non-Hermitian scattering symmetry revealed by diffusive channels**

Dong Wang<sup>1,2,3</sup>, Hongsheng Chen<sup>1,2,3\*</sup>, Cheng-Wei Qiu<sup>4\*</sup>, and Ying Li<sup>1,2,3\*</sup>

<sup>1</sup> *Interdisciplinary Center for Quantum Information, State Key Laboratory of Modern Optical Instrumentation, ZJU-Hangzhou Global Scientific and Technological Innovation Center, Zhejiang University, Hangzhou 310027, China*

<sup>2</sup> *International Joint Innovation Center, Key Lab. of Advanced Micro/Nano Electronic Devices & Smart Systems of Zhejiang, The Electromagnetics Academy of Zhejiang University, Zhejiang University, Haining 314400, China*

<sup>3</sup> *Jinhua Institute of Zhejiang University, Zhejiang University, Jinhua 321099, China*

<sup>4</sup> *Department of Electrical and Computer Engineering, National University of Singapore, Singapore 117583, Singapore*

\*e-mail: [chengwei.qiu@nus.edu.sg](mailto:chengwei.qiu@nus.edu.sg); \*e-mail: [hansomchen@zju.edu.cn](mailto:hansomchen@zju.edu.cn); \* e-mail: [eleying@zju.edu.cn](mailto:eleying@zju.edu.cn)

**The Hamiltonian interprets how the system evolves, while the scattering coefficients describe how the system responds to inputs. Recent studies on non-Hermitian physics have revealed many unconventional effects. However, in all cases, the non-Hermiticity such as material loss is only considered for the Hamiltonian, even when studying scattering properties. Another important component—the scattering channel, is always assumed to be lossless and time-reversal symmetric. This assumption hinders the exploration on the more general and fundamental properties of non-Hermitian scattering. Here, we identify a novel kind of scattering channel that obeys time-reversal anti-symmetry. Such diffusive scattering channels overturn the conventional understanding about scattering symmetry by linking the positive and negative frequencies. By probing non-Hermitian systems with the diffusive channels, we reveal a hidden anti-parity-time (APT) scattering symmetry, which is distinct from the APT symmetry of Hamiltonians studied before. The symmetric and symmetry broken scattering phases are observed for the first time as the collapse and revival of temperature oscillation. Our work highlights the overlooked role of scattering channels in the symmetry and phase transition of non-Hermitian systems, thereby gives the diffusion the new life as a signal carrier. Our findings can be utilized to the analysis and control of strongly dissipative phenomena such as heat transfer and charge diffusion.**

The investigation of scattering is of great prominence in physics research, because it could reveal fundamental properties about the scatterer, such as its symmetry. To the purpose, a common belief is that the incident and scattered signals should ideally not be further modified by the scattering channels that carry them. Therefore, most previous works based their analysis on the assumption of lossless scattering channels. Inside a lossless channel, a wave field  $F$  would commonly satisfy the time-reversal (T) symmetric wave equation  $\partial_t^2 F = a^2 \nabla^2 F$ , where  $a$  is a real

parameter, and  $\nabla^2$  is the Laplacian operator. The T-symmetry is reflected in the dispersion relation as shown in Fig. 1(a) and (b) (black and gray lines), where all the wavenumbers are purely real. The time-reversal operation maps the state with positive wavenumber  $k_c$  to that with  $-k_c$ . With the advent of non-Hermitian physics [1]-[6], it was recently realized that lossy systems can exhibit intriguing novel effects such as enhanced sensing capability [7]-[11], loss-induced lasing [12]-[14], non-reciprocal transmission [15]-[18], coherent perfect absorption [19]-[21], cloaking [22], etc. However, the studies on non-Hermitian scattering have long been captivated by the assumption of lossless scattering channels. The significance of the non-Hermiticity of the scattering channel has thus been completely overlooked so far.

Here, we made an in-depth analysis on the interplay between the scattering channels and the scatterer, which is manifested in the dispersion relation. In particular, we report a distinct kind of scattering channels which is lossy, and satisfies time-reversal anti-symmetry (anti-T-symmetry), rather than being T-symmetric. Mathematically, anti-T-symmetry requires that the channel's Hamiltonian  $H_c$  and the time-reversal operator  $\mathcal{T}$  are anti-commutation  $\{H_c, \mathcal{T}\} = 0$ . The feature may appear strange, but it can be shown to have a clear and fundamental physical origin. To see this, note that if we change the second-order time derivative in the wave equation to a first-order time derivative,  $\partial_t^2 F \rightarrow \partial_t F$ , the Hamiltonian  $H_c = ia^2 \nabla^2$  exactly obeys anti-T-symmetry. The resultant governing equation:  $\partial_t F = a^2 \nabla^2 F$ , is nothing but the diffusion equation with  $a^2 = D$  being the diffusivity. Therefore, the anti-T-symmetry actually describes the extreme case of field evolution in a purely lossy media, namely the diffusion process.

The anti-T-symmetric dispersion is shown in Fig. 1(a) and (b) (red and blue lines). Since the wavenumbers are complex for real frequencies, time-reversal operation maps  $k_c$  to  $-k_c^*$ . It is worth noting that the state under time-reversal operation does not fall on the dispersion curve of

the scattering channel at equal frequency, which instead goes to another branch at negative frequency [23]. This indicates that the time-reversal operation on fields in anti-T symmetric channels acts as a linkage between positive and negative frequencies. Fig. 1(c) and (d) demonstrate the effects and differences of time-reversal operation on the physical fields in the T-channel and anti-T-channel. For the first time, we show that the peculiar trait of anti-T-channel will reveal a series of novel scattering effects for non-Hermitian systems.

Previous studies considering lossless scattering channels fail to reveal some symmetries in non-Hermitian systems. Anti-parity-time (APT) symmetry defined by  $\{PT, H\} = 0$  is such a kind of typical non-Hermitian symmetries. Such Hamiltonians have aroused great interests [24]-[32], leading to the discoveries of novel effects including chiral mode switching [24], non-Hermitian topology [25],[26], sensing [27] and heat locking effect [28]. However, all existing works either only focus on isolated systems (Fig. 2(a)), or forcefully assume the channels to be T-symmetric (Fig. 2(b)). We find a clear distinction between the symmetry of the Hamiltonian and the symmetry of the scattering, as shown in the scenario of Fig. 2(a) and 2(b). That explains why previous works only use the scattering coefficient to reflect the symmetry of scatterer's Hamiltonian, but scattering symmetry at the entire system level cannot be manifested.

We reveal a unique scattering symmetry of APT systems preserved by the unusual feature of anti-T-symmetric, or diffusive channels (Fig. 2(c)). The symmetry of scattering is essentially different from the symmetry of a Hamiltonian. The symmetric and symmetry broken scattering phases are demonstrated with the distinguished behaviors in field evolutions. In addition, we find a specific excitation frequency at which the scattering is always in the symmetry-broken phase. Such a thresholdless symmetry-breaking feature indicates a mode decoupling under infinitesimal

perturbations, which is a unique feature brought by the signal, rather than by the system properties.

Here, without loss of generality, we use heat transfer system, a typical diffusive process, to study the properties of anti-T channel. Heat transfer plays a key role in energy transport. The huge demand for novel heat transfer functions in the industry and the accumulation of scientific research tools have stimulated the emerging of thermal metamaterial [33],[34]. Recently, non-Hermitian physics paved a new path to manipulating heat flux with metamaterials [21],[35]-[43] with extraordinary properties like thermal coherent perfect absorption [21], topological transition [35]-[37], thermal diode [38], localized heat diffusion [39],[40], phase oscillation [41], and diffusive skin effect [42],[43]. Despite these works, the non-Hermitian scattering of heat transfer has not been studied yet, due to the insurmountable obstacle of decomposing the temperature field into meaningful heat signals. Inspired by the special dispersion of anti-T channel, we overcome this challenge by introducing real-number frequency to heat signals [38] (Conventionally, the “frequency” of the temperature field is treated as purely imaginary [39],[40]). The heat signal with real-number frequency is constructed by the rotating heat source illustrated in Fig. 2(d). It can be proved (Supplementary Material) that the rotation directions are equivalent to the positive and negative frequencies. This treatment provides us the possibility to define chirality in heat signal. Like the circularly polarization of electromagnetic field in T-symmetric channels (Fig. 2(e)), we could design a special kind of signal with chirality (Fig. 2(f)), which is excited by our proposed rotating chiral heat source. The dipole in cross section (Supplementary Material):

$$\mathbf{p}_T = \iint \mathbf{r} \sigma_T dS = i \iint x \sigma_T dS + j \iint y \sigma_T dS \quad (1)$$

where  $\sigma_T$  is the temperature configuration in cross section. The sign changing of frequency results in the flip of chirality (e.g., from LCP to RCP in Fig. 1(c)), which can directly reflect the effect of the time-inversion operation.

The general heat transfer system is generated by the fixed temperature heat source, which only provides a steady heat flow without carrying any other information about heat signal. However, our above design introduces a time-harmonic oscillating heat source with the concept of chirality, enriching additional degrees of freedom to manipulate heat signal and investigate the propagating or scattering properties of field in anti-T channels. It is found that, when a thermally conductive cylinder is in contact with a rotating heat source as shown in Fig .1(b), the temperature distribution in the cylinder satisfies the form of a time-harmonic temperature field (Supplementary Materials):  $T_c(z, \phi, t) = F_c(z)e^{i\phi - i\omega t}$ . Here we have postulated that the medium is homogeneous along the radial direction provided that the cylinder's thickness is small. Then we let the space-dependent part  $F_c(z)$  has a fundamental solution of wave-like form:

$$F_c(z) = B_{c+}e^{ik_c z} + B_{c-}e^{-ik_c z} \quad (2)$$

By substituting  $T_c(z, \phi, t)$  into the heat diffusion equation  $\partial_t T_c = D\partial_z^2 T_c$  ( $D$  is the thermal diffusivity), we can calculate the wavenumber  $k_c$  in anti-T channel.  $B_{c+}$ , and  $B_{c-}$  can be complex numbers to incorporate phases in the fields. This treatment lets the temperature fields in anti-T channel have the form of 1D wave scattering, making the heat that is originally thought to be lacking degrees of freedom come alive at the signal level. As an exemplary case to illustrate the scattering features of anti-T channel, we consider the scatterers composed of spinning units, which are presented in the insets of Figs. 3(a) and (b). With thermal scattering theory (Supplementary Material), we could obtain the transmission spectra of the scatterers, as shown in the colored lines in Figs. 3(a) and (b). We have to mention that due to the spinning structure, the

transmission coefficient in negative frequency (light blue area) describes the transmission of opposite input in positive frequency indeed.

For clockwise (CW) rotating ring, Fig. 3(a) shows that  $t(-\omega) \neq t(\omega)$ , which can be explained by the structural asymmetry of this rotator. In addition, we find there is resonance point in the curve and it moves with different angular velocity. However, the resonance point is not equal to  $\Omega$  and we infer the reason is the coupling between spinner and channels. To illustrate this, we give Fig. 3(c). Despite the inequivalence between resonance frequency and angular velocity, there exists a linear relationship between them, which reflects system's resonant features.

Two coupled resonators could form an APT symmetric system with eligible coupling strength [32]. By combining the CW spinner with CCW spinner, the APT scatterer is generated [28]. Our calculation shows that  $t(-\omega) = t(\omega)$ , which is different from the case in a single rotor. Similar to the case of a single ring, resonance points are observed in the transmission spectrum of this APT scatterer. For APT system, there exists a splitting of the eigenspectrum of Hamiltonian, corresponding to the phase transition [26]. Therefore, we expect the peak frequencies of transmission coefficients to be predicted by the eigenfrequencies of this system which is related to system's Hamiltonian. Specifically, the real parts of Hamiltonian's eigenvalues correspond to transmission coefficients' peaks. Here, we conducted this analysis and discovered that, despite the existence of this trend, there is no obvious splitting and phase transition, which is shown in Fig. 3(d). This discrepancy was discussed in a previous work [44] and we reproduce this phenomenon in the diffusive system. However, the deeper physics behind it has not yet been revealed and the phase transition relating to scattering needs to be further studied and discussed.

For general two-port thermal scattering, temperature field in channels has the form  $T_{ci} = [A_i u_i^{\text{in}}(z, \omega) + B_i u_i^{\text{out}}(z, \omega)]$ ,  $u_i^{\text{in}}(z, \omega)$ ,  $u_i^{\text{out}}(z, \omega)$  are incoming mode and outgoing mode and  $A_i$ ,  $B_i$  are amplitudes of them respectively.  $A_i$  and  $B_i$  are connected with scattering matrix  $\mathbf{S}(\omega)$ ,  $\mathbf{B} = \mathbf{S}(\omega)\mathbf{A}$ .  $\mathbf{A} = [A_1, A_2]^T$  and  $\mathbf{B} = [B_1, B_2]^T$ . By applying PT operators on both sides of  $T_c$ , we eventually have the form (see Supplementary Material)  $(\mathcal{PT} T_c)_i = [(\mathcal{PT} \mathbf{A})_i u_i^{\text{in}}(z, -\omega) + (\mathcal{PT} \mathbf{B})_i u_i^{\text{out}}(z, -\omega)]$ , where  $\mathbf{T}_c = [T_{c1}, T_{c2}]^T$ . For APT symmetric systems, if there is an eigenstate  $T_{ci}$  at  $\omega$ , there must be another eigenstate  $(\mathcal{PT} T_c)_i$  at  $-\omega^*$ . Here, since  $\omega$  is real, the temperature field undergoing PT transformation should have another scattering relationship characterized by  $\mathbf{S}(-\omega)$ , where  $(\mathcal{PT})\mathbf{B} = \mathbf{S}(-\omega)(\mathcal{PT})\mathbf{A}$ . Combining the two scattering relations, we get the symmetry of scattering matrix in APT systems, which will build a bridge linking positive and negative frequencies:

$$(\mathcal{PT})\mathbf{S}(\omega)(\mathcal{PT})^{-1} = \mathbf{S}(-\omega) \quad (3)$$

The symmetry of scattering in APT systems is deposited into two matrices with positive and negative frequencies. This is one reason why the study on genuine APT scattering is few and arduous.

To demonstrate the complete symmetry of scattering matrix, a new matrix  $\mathbf{S}^4$  is proposed:

$$\begin{bmatrix} B_{1L} \\ B_{2L} \\ B_{1R} \\ B_{2R} \end{bmatrix} = \mathbf{S}^4 \begin{bmatrix} A_{1L} \\ A_{2L} \\ A_{1R} \\ A_{2R} \end{bmatrix} = \begin{bmatrix} 0 & S_{12}(-\omega) & S_{11}(-\omega) & 0 \\ S_{21}(\omega) & 0 & 0 & S_{22}(\omega) \\ S_{11}(\omega) & 0 & 0 & S_{12}(\omega) \\ 0 & S_{22}(-\omega) & S_{21}(-\omega) & 0 \end{bmatrix} \begin{bmatrix} A_{1L} \\ A_{2L} \\ A_{1R} \\ A_{2R} \end{bmatrix} \quad (4)$$

Here, subscripts  $L$  and  $R$  represent helicity of incoming and outgoing modes. With relation in Eq. , a symmetry has been found for  $\mathbf{S}^4$ :



$$(\mathcal{PT})\mathcal{S}^4(\omega)(\mathcal{PT})^{-1} = \mathcal{S}^4(\omega) \quad (5)$$

This suggests the invariance for  $\mathcal{S}^4$  under PT operation in APT systems. To reveal this property, eigenvalues  $s$  of  $\mathcal{S}^4$  are determined by the following formula:

$$s^2 = \text{Re}(r_{11}r_{22}^*) \pm \sqrt{-\text{Im}(r_{11}r_{22}^*)^2 + |t|^4} \quad (6)$$

Here, we have used relations in Eq. .

The eigenvalue spectrums to  $\mathcal{S}^4$  are given in Fig. 4(a) and Fig. 4(b). With eigenspectrum, symmetric phase and symmetry-broken phase to scattering are defined. In scattering symmetric phase, the eigenvalues for  $\mathcal{S}^4$  are totally real numbers while symmetry-broken phase for scattering implicates the appearance to imaginary parts of matrix's eigenvalues. This nature of phase transition is uncovered in Eq. . In addition, besides  $\omega$ ,  $\Omega$  serves as another modulation tool for scattering. The dependence of symmetry on parameters are summarized in the phase diagram in Fig. 4(c). Surprisingly, we notice that there is a special frequency, at which the scattering symmetry is always broken regardless of the rotation speed of the system. It could be seen from Eq. that at this special frequency,  $|t|^4 = [\text{Im}(r_{11}r_{22})]^2$  when  $\Omega = 0$  and  $|t|^4 < [\text{Im}(r_{11}r_{22})]^2$  when  $\Omega \neq 0$ . The emergence of rotation is responsible for the scattering symmetry-breaking. Considering  $\mathcal{S}^4$  involves the integral information of this APT symmetric scattering system, this thresholdless symmetry-broken phenomenon could be interpreted as the signal-induced decoupling of the coupled system. This is quite counterintuitive. Because most of coupled systems has a critical coupling, only when the coupling exceeds this value can the coupling be decoupled and the symmetry breaking state is achieved.

Furthermore, we also study the eigenstates of  $\mathcal{S}^4$ . Another physical quantity named temperature amplitude ratio (TAR) is proposed to quantify the intensity relation between scattering ports, defined as:  $\text{TAR} = \text{TA}_r/\text{TA}_l$ , which means the ratio of temperature amplitude

(represents field intensity) for right and left interfaces (scattering ports) in Fig. 3(b). When the input is the eigenstate of  $\mathcal{S}^4$ , we have the input vector:  $\Psi_{\text{in}} = (s_{1L}e^{-i\omega t}, s_{2L}e^{i\omega t}, s_{1R}e^{i\omega t}, s_{2R}e^{-i\omega t})^T$ . The output vector  $\Psi_{\text{out}}$  is obtained by scattering matrix  $\mathcal{S}^4$ :  $\Psi_{\text{out}} = \mathcal{S}^4\Psi_{\text{in}}$ . Since the temperature fields for left and right ports are the combinations of respective input and output components, the amplitudes are  $\text{TA}_l = |\psi_{\text{in}1} + \psi_{\text{in}3} + \psi_{\text{out}1} + \psi_{\text{out}3}|$  and  $\text{TA}_r = |\psi_{\text{in}2} + \psi_{\text{in}4} + \psi_{\text{out}2} + \psi_{\text{out}4}|$ . Our calculation has shown diverse features for TAR under different incident scattering eigenstates. When the incident eigenstate is in symmetric phase, the TAR keeps a constant 1, which reflects the symmetric scattering, as shown in Fig. 4(d). When the incident eigenstate is in symmetry-broken phase, the stability of TAR is disrupted and it presents oscillation in time domain, as depicted in Fig. 4(e). In addition, we investigate the phase shift of the temperature dipole in the left and right ports,  $\delta\theta = \text{angle}(\mathbf{P}_{Tr}) - \text{angle}(\mathbf{P}_{Tl})$ , to represent phase information. We find it shows different behaviors in different phases as well. Fig. 4(d) and (e) exhibit this phenomenon with numerical and simulation results. Notably, the TAR represents the intensity relation between two scattering ports, we conclude that symmetry in scattering plays a role in maintaining the intensity stability during scattering process. Furthermore, a more vivid dynamic result of the TAR is given in Fig. 4(f). This figure exhibits the behavior of TAR from symmetry broken phase to symmetric phase.

The scattering problem of non-Hermitian system carried by time-reversal anti-symmetric (anti-T) channel is considered for the first time in our work. We constructed a theoretical scattering model of the signal propagating in this anti-T channel. With the unusual feature of anti-T scattering channel, we revealed the scattering symmetry of APT system characterized by scattering matrix that associates positive frequency with negative frequency, which attributes a

remarkable distinction to PT systems. Furthermore, we observed different scattering phases with distinguishing phenomena corresponding to the stability of temperature amplitude ratio. Our work is of great significance to the study of non-Hermitian physics, non-Hermitian symmetry, scattering, heat transfer, and many other related fields. It also implies tremendous applicational possibilities in the manipulation of various strongly dissipative phenomena such as heat transfer and charge diffusion.

## References

- [1] M.-A. Miri and A. Alù, Exceptional Points in Optics and Photonics, *Science* **363**, 6422 (2019).
- [2] Y. Ashida, Z. Gong, and M. Ueda, Non-Hermitian Physics, *Advances in Phys.* **69**, 249 (2020).
- [3] Z. Li, G. Cao, C. Li, S. Dong, Y. Deng, X. Liu, J. S. Ho, and C.-W. Qiu, Non-Hermitian Electromagnetic Metasurfaces at Exceptional Points (Invited Review), *Prog. Electromagn. Res.* **171**, 1 (2021).
- [4] R. El-Ganainy, K. G. Makris, M. Khajavikhan, Z. H. Musslimani, S. Rotter, and D. N. Christodoulides, Non-Hermitian Physics and PT Symmetry, *Nat. Phys.* **14**, 11 (2018).
- [5] Ş. K. Özdemir, S. Rotter, F. Nori, and L. Yang, Parity–Time Symmetry and Exceptional Points in Photonics, *Nat. Mater.* **18**, 783 (2019).
- [6] S. K. Gupta, Y. Zou, X. Zhu, M. Lu, L. Zhang, X. Liu, and Y. Chen, Parity-Time Symmetry in Non-Hermitian Complex Optical Media, *Adv. Mater.* 1903639 (2019).
- [7] W. Chen, Ş. Kaya Özdemir, G. Zhao, J. Wiersig, and L. Yang, Exceptional Points Enhance Sensing in an Optical Microcavity, *Nature* **548**, 192 (2017).

- [8] H. Hodaei, A. U. Hassan, S. Wittek, H. Garcia-Gracia, R. El-Ganainy, D. N. Christodoulides, and M. Khajavikhan, Enhanced Sensitivity at Higher-Order Exceptional Points, *Nature* **548**, 187 (2017).
- [9] P.-Y. Chen, M. Sakhdari, M. Hajizadegan, Q. Cui, M. M.-C. Cheng, R. El-Ganainy, and A. Alù, Generalized Parity–Time Symmetry Condition for Enhanced Sensor Telemetry, *Nat. Electron.* **1**, 297 (2018).
- [10] H. Ma, D. Li, N. Wu, Y. Zhang, H. Chen, and H. Qian, Nonlinear All-Optical Modulator Based on Non-Hermitian PT Symmetry, *Photon. Res.* **10**, 980 (2022).
- [11] R. Kononchuk, J. Cai, F. Ellis, R. Thevamaran, and T. Kottos, Exceptional-Point-Based Accelerometers with Enhanced Signal-to-Noise Ratio, *Nature* **607**, 7920 (2022).
- [12] B. Peng, Ş. K. Özdemir, S. Rotter, H. Yilmaz, M. Liertzer, F. Monifi, C. M. Bender, F. Nori, and L. Yang, Loss-Induced Suppression and Revival of Lasing, *Science* **346**, 328 (2014).
- [13] L. Feng, Z. J. Wong, R.-M. Ma, Y. Wang, and X. Zhang, Single-Mode Laser by Parity-Time Symmetry Breaking, *Science* **346**, 972 (2014).
- [14] H. Hodaei, M.-A. Miri, M. Heinrich, D. N. Christodoulides, and M. Khajavikhan, Parity-Time–Symmetric Microring Lasers, *Science* **346**, 975 (2014).
- [15] A. Regensburger, C. Bersch, M.-A. Miri, G. Onishchukov, D. N. Christodoulides, and U. Peschel, Parity–Time Synthetic Photonic Lattices, *Nature* **488**, 167 (2012).
- [16] Z. Lin, H. Ramezani, T. Eichelkraut, T. Kottos, H. Cao, and D. N. Christodoulides, Unidirectional Invisibility Induced by PT-Symmetric Periodic Structures, *Phys. Rev. Lett.* **106**, 213901 (2011).
- [17] L. Zhang et al., Acoustic Non-Hermitian Skin Effect from Twisted Winding Topology, *Nat. Commun.* **12**, 6297 (2021).

- [18] B. Peng, Ş. K. Özdemir, F. Lei, F. Monifi, M. Gianfreda, G. L. Long, S. Fan, F. Nori, C. M. Bender, and L. Yang, Parity–Time-Symmetric Whispering-Gallery Microcavities, *Nat. Phys.* **10**, 394 (2014).
- [19] W. Wan, Y. D. Chong, L. Ge, H. Noh, A. D. Stone, and H. Cao, Time-Reversed Lasing and Interferometric Control of Absorption, *Science* **331**, 889 (2011).
- [20] Y. D. Chong, L. Ge, and A. D. Stone, P T -Symmetry Breaking and Laser-Absorber Modes in Optical Scattering Systems, *Phys. Rev. Lett.* **106**, 093902 (2011).
- [21] Y. Li, M. Qi, J. Li, P.-C. Cao, D. Wang, X.-F. Zhu, C.-W. Qiu, and H. Chen, Heat Transfer Control Using a Thermal Analogue of Coherent Perfect Absorption, *Nat. Commun.* **13**, 2683 (2022).
- [22] R. Fleury, D. Sounas, and A. Alù, An Invisible Acoustic Sensor Based on Parity-Time Symmetry, *Nat. Commun.* **6**, 5905 (2015).
- [23] G. Rousseaux, C. Mathis, P. Maïssa, T. G. Philbin, and U. Leonhardt, Observation of Negative-Frequency Waves in a Water Tank: A Classical Analogue to the Hawking Effect?, *New J. Phys.* **10**, 053015 (2008).
- [24] X.-L. Zhang, T. Jiang, and C. T. Chan, Dynamically Encircling an Exceptional Point in Anti-Parity-Time Symmetric Systems: Asymmetric Mode Switching for Symmetry-Broken Modes, *Light Sci. Appl.* **8**, 88 (2019).
- [25] H. C. Wu, L. Jin, and Z. Song, Topology of an Anti-Parity-Time Symmetric Non-Hermitian Su-Schrieffer-Heeger Model, *Phys. Rev. B* **103**, 235110 (2021).
- [26] A. Bergman, R. Duggan, K. Sharma, M. Tur, A. Zadok, and A. Alù, Observation of Anti-Parity-Time-Symmetry, Phase Transitions and Exceptional Points in an Optical Fibre, *Nat. Commun.* **12**, 486 (2021).

- [27] H. Qin, Y. Yin, and M. Ding, Sensing and Induced Transparency with a Synthetic Anti-PT Symmetric Optical Resonator, *ACS Omega* **6**, 5463 (2021).
- [28] Y. Li, Y.-G. Peng, L. Han, M.-A. Miri, W. Li, M. Xiao, X.-F. Zhu, J. Zhao, A. Alù, S. Fan, and C.-W. Qiu, Anti-Parity-Time Symmetry in Diffusive Systems, *Science* **364**, 170 (2019).
- [29] P. Peng, W. Cao, C. Shen, W. Qu, J. Wen, L. Jiang, and Y. Xiao, Anti-Parity-Time Symmetry with Flying Atoms, *Nat. Phys.* **12**, 1139 (2016).
- [30] Y. Choi, C. Hahn, J. W. Yoon, and S. H. Song, Observation of an Anti-PT-Symmetric Exceptional Point and Energy-Difference Conserving Dynamics in Electrical Circuit Resonators, *Nat. Commun.* **9**, 2182 (2018).
- [31] Y. Jiang, Y. Mei, Y. Zuo, Y. Zhai, J. Li, J. Wen, and S. Du, Anti-Parity-Time Symmetric Optical Four-Wave Mixing in Cold Atoms, *Phys. Rev. Lett.* **123**, 193604 (2019).
- [32] H. Zhang, R. Huang, S.-D. Zhang, Y. Li, C.-W. Qiu, F. Nori, and H. Jing, Breaking Anti-PT Symmetry by Spinning a Resonator, *Nano Lett.* **20**, 7594 (2020).
- [33] S. Yang, J. Wang, G. Dai, F. Yang, and J. Huang, Controlling Macroscopic Heat Transfer with Thermal Metamaterials: Theory, Experiment and Application, *Phys. Rep.* **908**, 1 (2021).
- [34] Y. Li, W. Li, T. Han, X. Zheng, J. Li, B. Li, S. Fan, and C.-W. Qiu, Transforming Heat Transfer with Thermal Metamaterials and Devices, *Nat. Rev. Mater.* **6**, 488 (2021).
- [35] G. Xu, Y. Li, W. Li, S. Fan, and C.-W. Qiu, Configurable Phase Transitions in a Topological Thermal Material, *Phys. Rev. Lett.* **127**, 105901 (2021).
- [36] G. Xu, Y. Yang, X. Zhou, H. Chen, A. Alù, and C.-W. Qiu, Diffusive Topological Transport in Spatiotemporal Thermal Lattices, *Nat. Phys.* **18**, 4 (2022).

- [37] G. Xu, W. Li, X. Zhou, H. Li, Y. Li, S. Fan, S. Zhang, D. N. Christodoulides, and C.-W. Qiu, Observation of Weyl Exceptional Rings in Thermal Diffusion, *Proc. Natl. Acad. Sci. U.S.A.* **119**, e2110018119 (2022).
- [38] Y. Li, J. Li, M. Qi, C.-W. Qiu, and H. Chen, Diffusive Nonreciprocity and Thermal Diode, *Phys. Rev. B* **103**, 014307 (2021).
- [39] M. Qi, D. Wang, P.-C. Cao, X.-F. Zhu, C.-W. Qiu, H. Chen, and Y. Li, Geometric Phase and Localized Heat Diffusion, *Adv. Mater.* **34**, 2202241 (2022).
- [40] H. Hu et al., Observation of Topological Edge States in Thermal Diffusion, *Adv. Mater.* **34**, 2202257 (2022).
- [41] P.-C. Cao, Y. Li, Y.-G. Peng, C.-W. Qiu, and X.-F. Zhu, High-Order Exceptional Points in Diffusive Systems: Robust APT Symmetry Against Perturbation and Phase Oscillation at APT Symmetry Breaking, *ES Energy Environ.* **7**, 48 (2019).
- [42] P.-C. Cao, Y. Li, Y.-G. Peng, M. Qi, W.-X. Huang, P.-Q. Li, and X.-F. Zhu, Diffusive Skin Effect and Topological Heat Funneling, *Commun. Phys.* **4**, 1 (2021).
- [43] P.-C. Cao, Y.-G. Peng, Y. Li, and X.-F. Zhu, Phase-Locking Diffusive Skin Effect, *Chin. Phys. Lett.* **39**, 57801 (2022).
- [44] Q. Geng and K.-D. Zhu, Discrepancy between Transmission Spectrum Splitting and Eigenvalue Splitting: A Reexamination on Exceptional Point-Based Sensors, *Photon. Res.* **9**, 1645 (2021).

## Acknowledgments

The work at Zhejiang University was sponsored by the National Natural Science Foundation of China (NNSFC) under Grants No. 92163123, 61625502, No.11961141010, and No. 61975176,

the Top-Notch Young Talents Program of China, and the Fundamental Research Funds for the Central Universities (2021FZZX001-19).

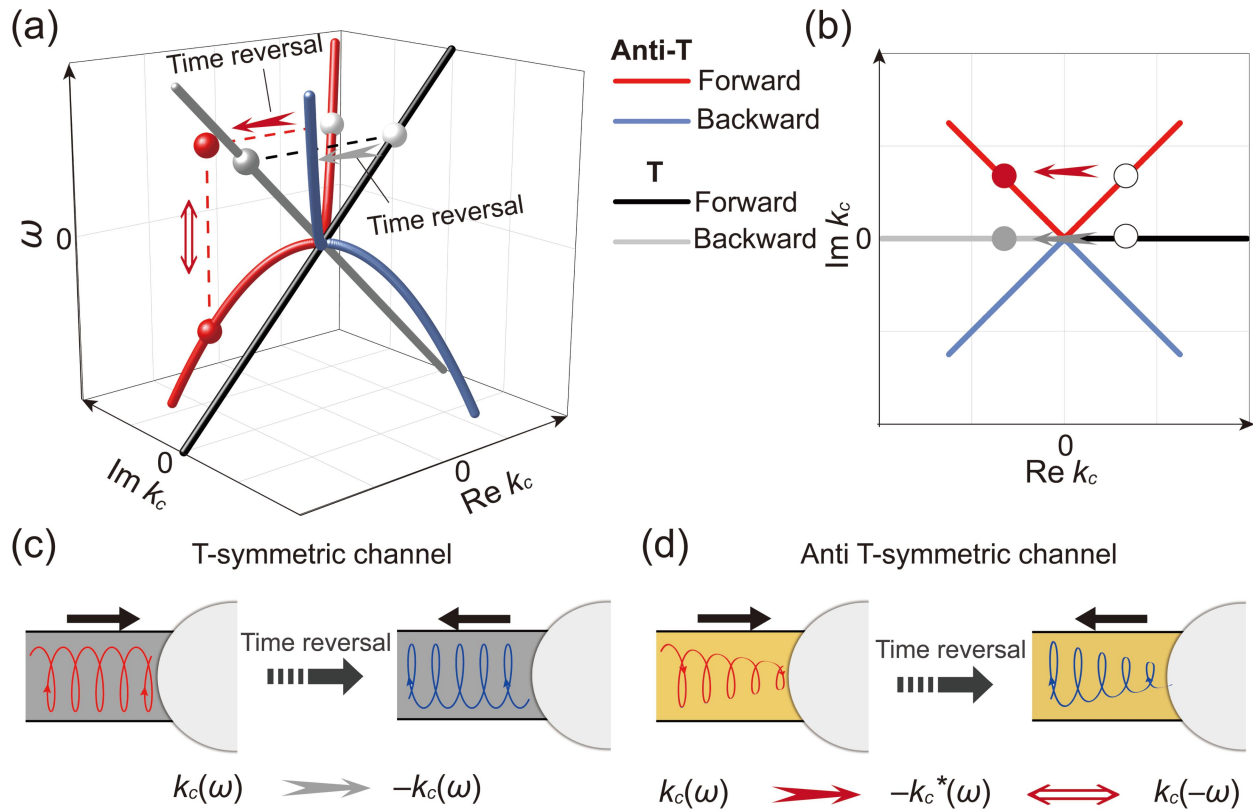


FIG. 1. Time-reversal in T-symmetric and anti T-symmetric channels. (a) Dispersion of time-harmonic field in anti T-symmetric (red or blue lines) and T-symmetric (black or gray lines) channel. The forward and backward modes are divided according to the positive and negative phase velocity  $v_p = \text{Re}(\omega)/\text{Re}(k_c)$ . The white balls are the initial states, the red and gray balls are the states after time-reversal operation. (b) Top view of the dispersion curves. (c) and (d) illustrate the physical field after time-reversal operation in T channel and anti-T channel.



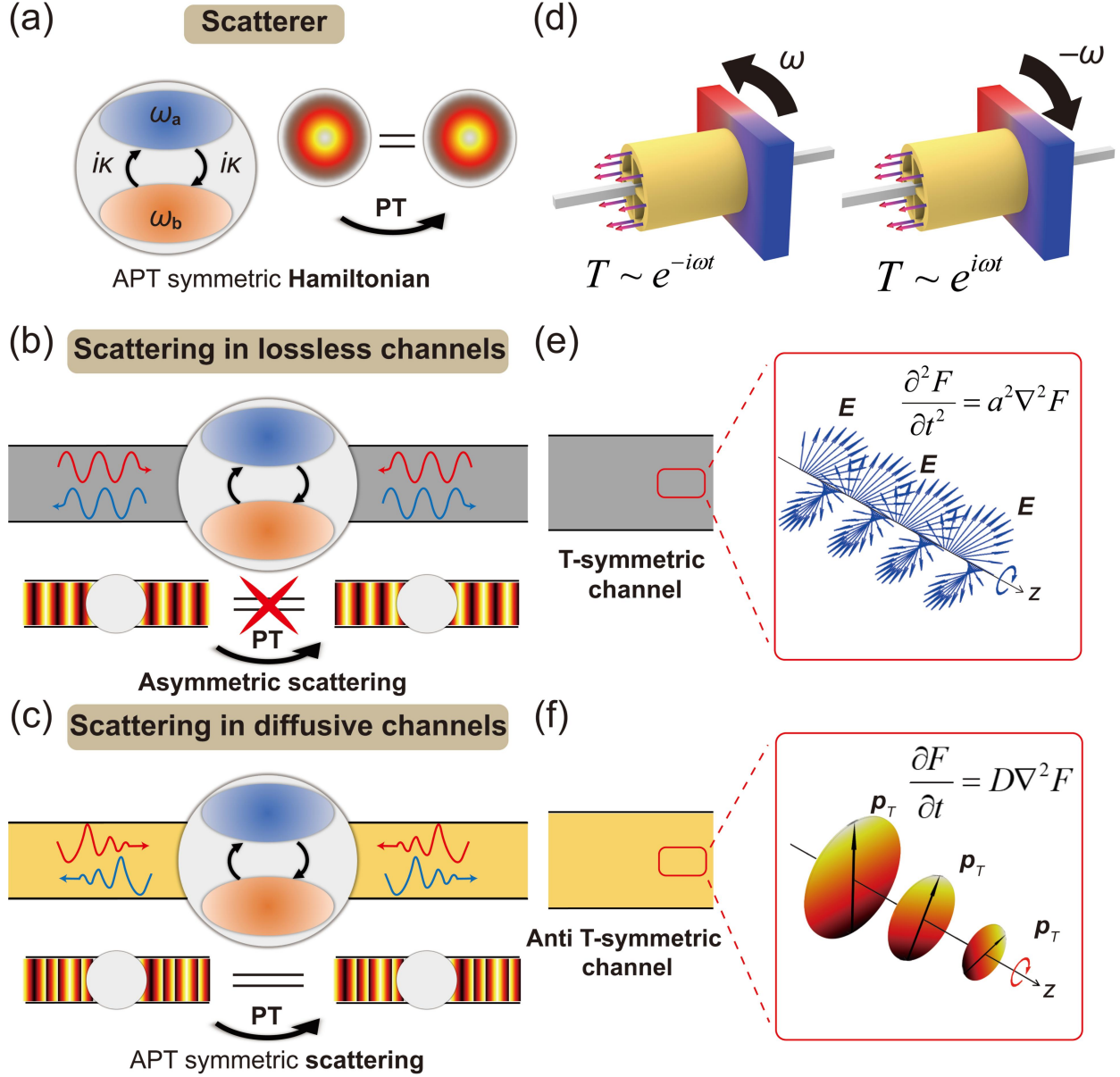


FIG. 2. Schematic of (a) scatterer with APT symmetric Hamiltonian (left) and the field (right). (b) Asymmetric scattering: APT scatterer with lossless channels (up) and the field (down). (c) APT symmetric scattering: APT scatterer with diffusive channels (up) and the field (down). (d) Experimental suggestion on the realization of positive and negative frequency in temperature field. (e) and (f) show the time harmonic fields propagating in T-symmetric (wave system) and anti T-symmetric channel (diffusive system).

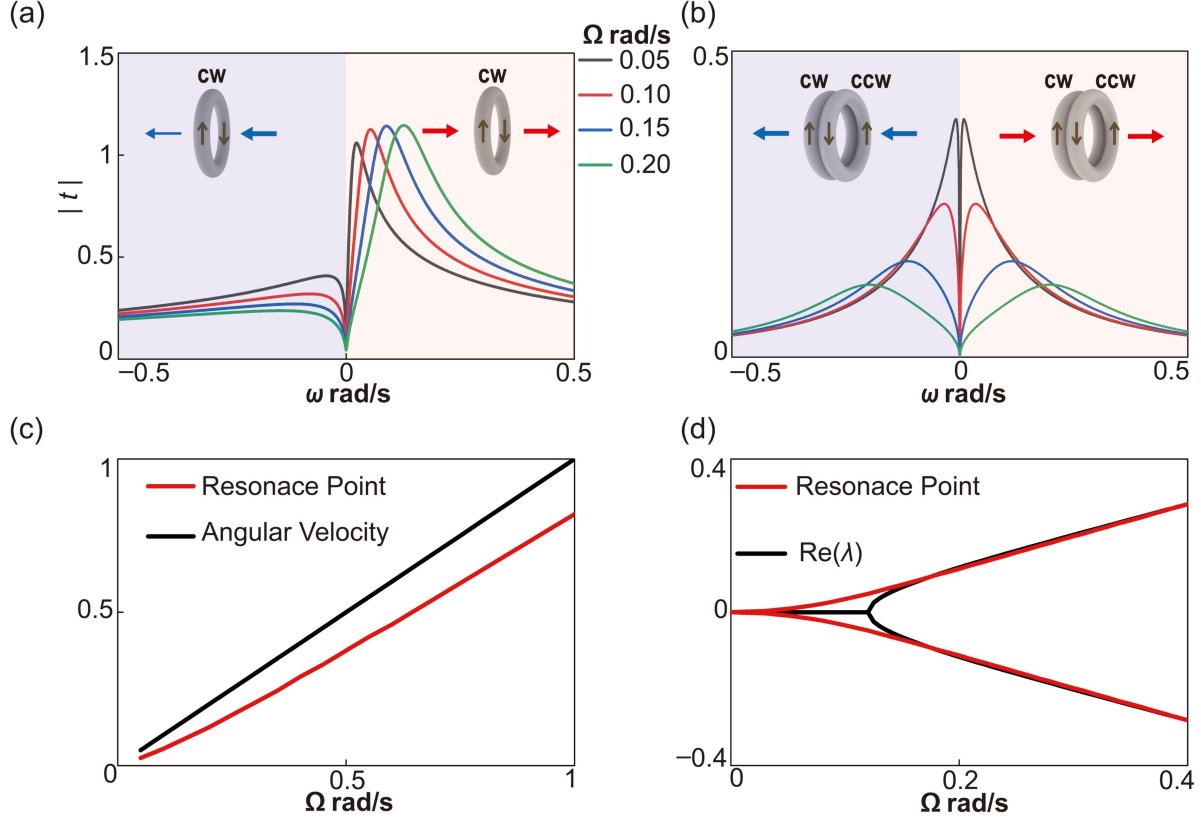


FIG. 3. Scattering in anti-T channels. (a) Transmission spectra of clockwise (CW) rotating ring. (b) Transmission spectra of coupled CW and CCW rotors (APT scatterer). Light blue (red) area in (a) and (b) represents the transmission for right to left (left to right), shown as the blue (red) arrows in the inset. (c) Resonance points of transmission spectra in (a) (red line) versus angular velocity (black line). (d) The correspondence between eigenvalues of scatterer's Hamiltonian and resonance points on transmission spectra in (b). Red line represents the resonance points in transmission curves. Black line indicates the real eigenspectrum to this APT scatterer's Hamiltonian.

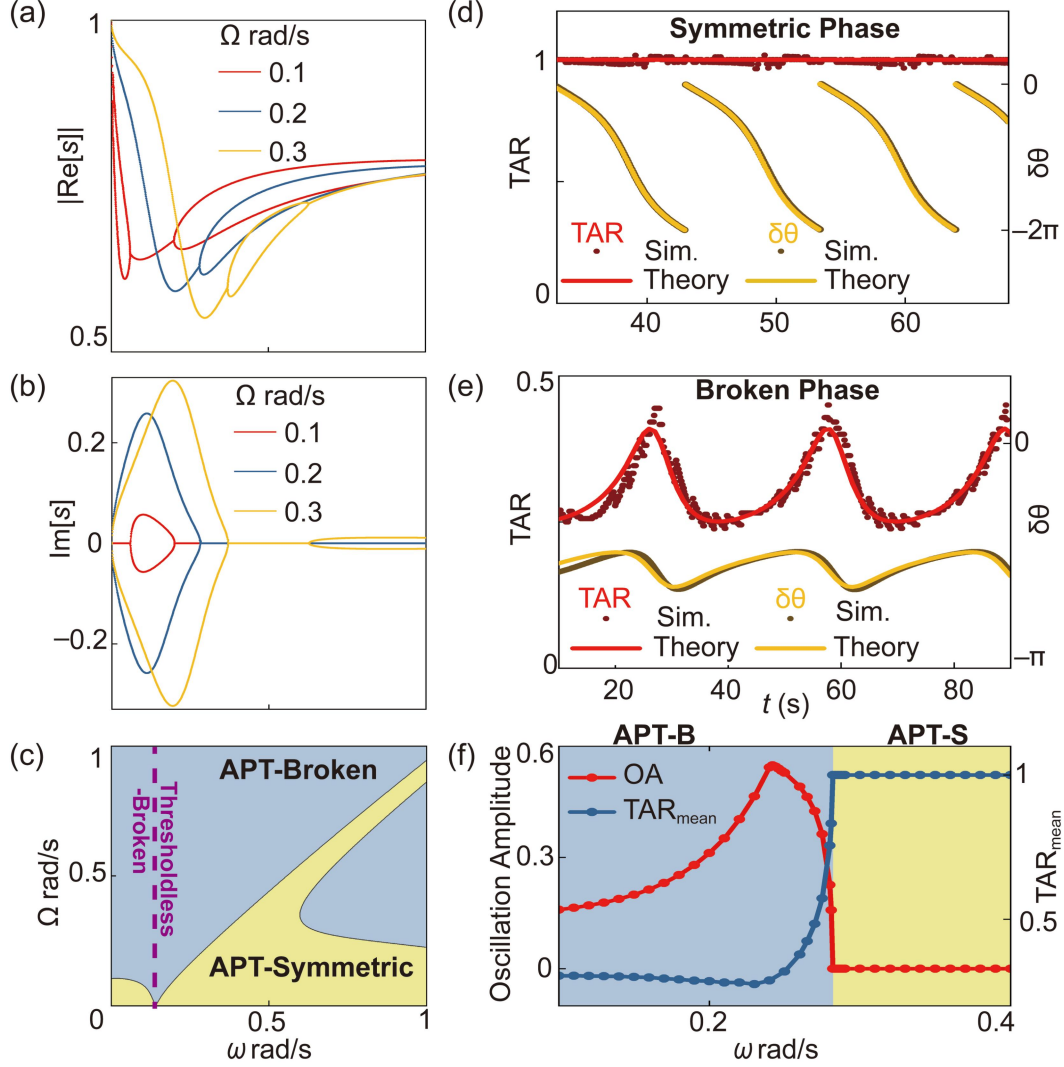


FIG. 4. Symmetry in scattering and the phase transition. (a) and (b) are the eigenspectra of scattering matrix  $\mathcal{S}^4$ . (c) Phase diagram of scattering matrix  $\mathcal{S}^4$ . Yellow and blue region correspond to scattering symmetric phase and scattering symmetry-broken phase respectively. The purple dotted line represents the thresholdless-broken region. (d) and (e) portray the time-domain transmission amplitude ratio (TAR) and phase shift ( $\delta\theta$ ) in symmetric / symmetry-broken phase.  $\omega$  and  $\Omega$  are (0.3, 0.2) and (0.1, 0.2) respectively. (f) Lines of oscillation amplitudes in TAR (red) and average values in TAR over a period (blue).  $\Omega = 0.2$  rad/s and  $\omega$  changes from 0.1 to 0.4 rad/s.